Guided-Mode Resonance Enhanced Ge-on-Si Self-Powered Surface Illuminated Photodetector for Ultrahigh-Speed Optical Communication Systems

Ahmad Lotfiani and Hamed Dehdashti Jahromi

***Abstract*—Germanium-on-Silicon photodetectors offer complementary metal-oxide-semiconductor (CMOS) compatibility and ultra-fast response, making them attractive for silicon photonics in the telecommunication band (O-band, 1310 nm). However, their low absorption coefficient in the near-infrared region (NIR) limits quantum efficiency. Here, we propose a high-performance Germanium photodetector on silicon that addresses this challenge. Our design incorporates a self-driven photovoltaic structure with an ultra-thin (100 nm) Ge absorption layer and a strategically placed silicon nanodisk array. This nanodisk array efficiently couples light into the device, leading to a significantly enhanced light–matter interaction and a remarkable improvement in external quantum efficiency (EQE) (74%) and responsivity (0.78 A/W) at 1310 nm. Additionally, the device exhibits an exceptional response time of 1.4 ps and a high photo-to-dark current ratio (3 × 10^{10}), demonstrating its suitability for high-speed NIR detection. The ultra-thin Ge layer and efficient light coupling pave the way for miniaturization and low-power operation, making this design promising for future high-performance NIR photodetectors.**

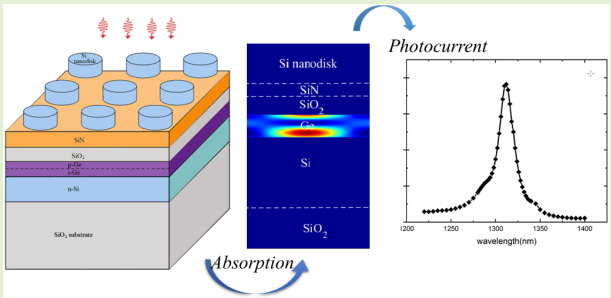

***Index Terms*—Ge-on-Si photodetector, high quantum efficiency, high speed, normal incidence, self-driven photovoltaic.**

I. Introduction

PHOTODETECTORS are electronic devices for converting optical signals into electrical signals [1], [2], [3]. In optical communication systems, photodetectors are used to receive signals transmitted through optical fibers. Infrared (IR) photodetectors have been widely used in diverse applications, including image sensing, optical communications, distance sensors, thermal imaging, night vision, fire mapping, space applications, and chemical analysis [4], [5], [6]. Particularly, the photodetectors working at wavelengths of 1310 nm (O band) and 1550 nm (C band) are important elements for optical communication [7], [8]. High cost, complicated fabrication procedures, and high dark current are the important bottlenecks limiting the development of IR photodetectors [9]. Different materials and structures of IR photodetectors have been proposed and developed for high-performance IR applications, such as InSb, and GaAs-based devices, colloidal quantum dot structure, and ternary compound semiconductors (HgCdTe, CdZnTe) photodetectors [10], [11], [12]. The fabrication complexity and process cost of these devices are not competitive compared to the complementary metal-oxide-semiconductor (CMOS)-compatible Silicon (Si)-based photodetectors. Matching the properties of optical and electronic devices, such as size, capacitance, and impedance, is a fundamental step toward improving the performance of nanoscale Ge photodetectors and developing more advanced optical processors. [13]. The CMOS-compatible Si-based photonic devices are promising platforms and have attracted great attention to producing low-power and compact circuits on the same chip of the microelectronic circuits [14]. While III-V compound semiconductors are not compatible with CMOS technology, they are currently the dominant platform for surface-illuminated photodetectors in the telecommunication window due to their low dark current and high quantum efficiency [15]. Although Group IV elements' indirect band gap prevents them from being used in semiconductor lasers [16], Si-Germanium (Ge) photodetectors [17], [18] are increasingly being utilized in optical communications. Ge-on-Si photodetectors are a

Received 4 October 2024; revised 20 October 2024; accepted 20 October 2024. Date of publication 29 October 2024; date of current version 13 December 2024. The associate editor coordinating the review of this article and approving it for publication was Dr. Juan A Lenero-Bardallo. *(Corresponding author: Hamed Dehdashti Jahromi.)*

The authors are with the Department of Engineering, Jahrom University, Jahrom, 7413188941 Fars, Iran (e-mail: jahromi@jahromu.ac.ir).

Digital Object Identifier 10.1109/JSEN.2024.3485510

1558-1748 © 2024 IEEE. Personal use is permitted, but republication/redistribution requires IEEE permission.
See https://www.ieee.org/publications/rights/index.html for more information.

Authorized licensed use limited to: Huazhong University of Science and Technology. Downloaded on December 06,2025 at 16:15:11 UTC from IEEE Xplore. Restrictions apply.

promising technology for optical communication in the O-band (1260–1360 nm) because of their high performance and cost-effectiveness.

Surface illumination, a technique that directs photons onto the device's surface, can improve Ge-on-Si photodetectors. This increases absorption efficiency and reduces noise, making it a promising approach despite higher costs. Ge-on-Si photodetectors, made by growing Ge on Si, convert light into electrical signals. Surface illumination improves their performance, but low optical absorption and external quantum efficiency (EQE) at the optical telecommunication band remain a challenge. [19]. The intrinsic absorption layer's thickness can generally be increased to enhance the responsivity as a general approach. However, this will limit the bandwidth of Ge photodetectors due to the long transit times of photogenerated carriers [20].

Ge-based photodetector with low responsivity at telecommunication wavelength was reported by Yang et al. [13] and the low responsivity was justified by the authors to the Ge low absorption coefficient at 1310 and 1550 nm. Plasmonic photodetectors are interesting due to their ability to light confining below the diffraction limit, which makes it possible for deep subwavelength light–matter interaction. This enables significant device size reduction, moving the technology one step closer to the fusion of electronic and optical components of the same size [21]. Yakimov et al. [22] reported the optical properties of stacking of self-assembled Ge quantum dots in a mid-infrared Ge/Si photodetector. The stack of self-assembled Ge quantum dots couple the incident light to the adjacent nanoplasmonic arrays of subwavelength holes in metallic films via near-field spectra. They found that the stack of self-assembled Ge quantum dots with nanoplasmonic arrays provides a great improvement in the normal-incident photoresponse of the photodetector through Rayleigh anomaly [22]. Chen et al. [23] designed and fabricated a Ge PIN photodetector on a Si substrate using a low-temperature Ge buffer layer technique. They introduced Si as a passivation layer between n^+-Ge and metal, providing a better ohmic contact. The device's characterizations demonstrated the 3 dB bandwidth of 4 GHz, and the optical responsivity is 0.1 A/W at the wavelength of 1.55 μm at a reverse bias voltage of 1 V [23]. Lin et al. [24] reported a normal incidence vertical Ge-on-SiO_2 PIN photodetector with ion implantation of arsenic and boron at the top and bottom of the Ge layer, respectively. The B-doped layer (p^+-contact) at the bottom of the Ge layer boosts the collection of photogenerated electron/hole pair more efficiently in the vertical electric field, which enhances the device's responsivity. Their device fabrication process is compatible with GOI platforms that enable the fabrication of CMOS-photonic devices. The device had responsivity of 0.39 A/W at 1550 nm and a −3 dB bandwidth of ∼32 GHz at 1 V reverse bias [24].

To address the quantum efficiency-bandwidth trade-off in normal incidence Ge photodetectors, a variety of strategies for increasing responsivity have been implemented. Liu et al. [20] designed a Ge/SiO_2 grating to enhance a thin-film Ge-on-Si-on-insulator photodetector. The grating coupled light efficiently, boosting absorption and bandwidth-efficiency product to 66 GHz. Zhao et al. [25] tried to improve the electrical characteristics of a Ge-on-SiO_2 PIN photodetectors by implementing better crystal quality and its optical performance through a better optical confinement and resonant cavity effect by integrating a tetraethylorthosilicate layer on the oxide substrate. They reported responsivity of 0.5 A/W for 1550 nm and 0.9 A/W for 1310 nm wavelength [25]. Double lateral silicon nitride waveguides for the Ge-on-Si photodiode concept were introduced by Hu et al. [26] for the first time. The double lateral waveguide configuration provides uniform optical field distribution in the photodiode's active region (Ge layer), which improves the characteristics of the photodetector specially its response times. The design device achieved responsivity of 0.52 A/W and the −3 dB bandwidth of 60 GHz at 3 V reverse bias voltage [26]. A hole array was added to the optical grating of a lateral Ge-on-insulator PIN photodetectors by Zhou et al. [27] to boost the optical absorption by guiding normal incident light's lateral propagation. Moreover, the hole-array structure also benefits the vertical resonance modes. The combination of hole-array and grating structure improved the photodetector's responsivity three times and bandwidth 1.6 times at 1550 nm in 5 V reverse bias voltage. The device's planar configuration is suitable for large-scale monolithic integration [27].

This paper presents a normal incidence Ge-on-Si PIN photodetector, which employs an optical structure to excite guided-mode resonance in a very thin i-region of the photodiode and enhance light absorption and, hence, the EQE. The thickness of the intrinsic Ge layer has a critical role in the performance of the Ge-on-Si PIN photodiode. This is a tradeoff between the device's photoresponse and electrical bandwidth, which is a big challenge for designers. In this design, the thickness of the intrinsic Ge layer is reduced to achieve higher electrical bandwidth while the degradation in the optical absorption is compensated by an optical structure and the silicon nanodisks arrays. The designed device can work in self-driven (self-powered) mode and high EQE of 74%, photo-to-dark current ratio of 3×10^{10}, and responsivity of 0.78 A/W are achieved at 1310 nm. The designed device has a 1.4 ps response time and a −3 dB bandwidth of 250 GHz, which is an excellent candidate for ultrahigh-speed optical communication. The metals' plasmonic effect is another approach for optimizing the absorption, but metal will bring additional heat energy and is incompatible with CMOS technology. The rest of this article is organized as follows. Section II presents the device structure in detail and a comprehensive description of simulation steps. The theoretical simulation and analyses of the device's performance are provided in Section III. In this section, the device's optical characteristics and electrical behavior are studied in detail separately. Finally, the conclusion ends the article in Section IV.

II. Design and Simulation

A. Device Structure

In this section, the proposed structure for the device is introduced and described. In Fig. 1, the 3-D schematic view of the designed device is presented. The device is a Ge-on-Si photonics PIN photodiode. SiO_2 layer with 1.33 μm thickness

Authorized licensed use limited to: Huazhong University of Science and Technology. Downloaded on December 06,2025 at 16:15:11 UTC from IEEE Xplore. Restrictions apply.

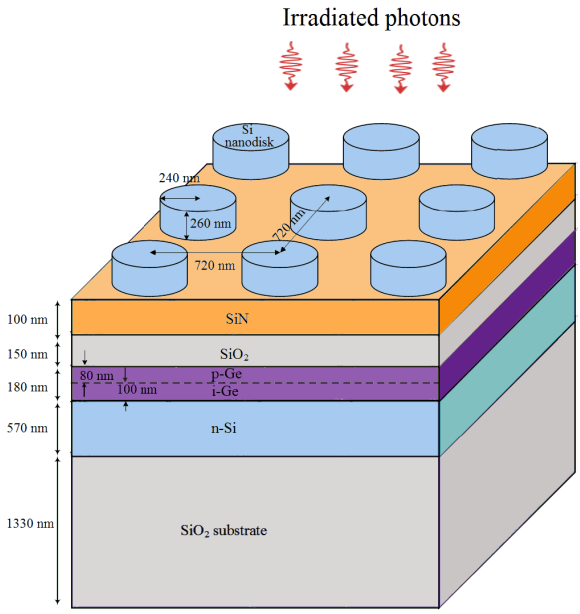

Fig. 1. Schematic view of the designed structure.

is selected as a substrate for deposition of the main layers of electronic and photonic parts of the device. A n-doped Si layer with 570 nm thickness and 6×10^{22} cm^{-3} impurity concentration is chosen to be on the SiO_2 substrate as the n-side of PIN junction. A 180-nm Ge layer is considered on the Si layer. The first 100 nm thickness of the germanium layer is an intrinsic region for the generation of electron-hole by absorbing the confined line in the region, and the remaining 80-nm thick Ge layer is doped with a p-type impurity by 3×10^{20} cm^{-3} concentration. Therefore, the PIN photodiode has an n-Si/i-Ge/p-Ge structure. These layers form the electrical structure of the PIN photodiode. The optical structure is designed to confine the irradiated photons at the desired wavelength in the i-region of the PIN photodiode, which increases light absorption by the photodetector and enhances the photo-to-dark current ratio, EQE, and responsivity of the designed device. The optical structure of the device is composed of a stack of SiO_2 and SiN (Si_3N_4) layers and periodic Si nanodisks on the electrical structure. The SiO_2 layer with a thickness of 150 nm is placed on the Ge layer, and a SiN layer with 100 nm thick is deposited on the SiO_2 layer. The high refractive Si nanodisks are arranged on the SiN layer in the same period in the x and y directions and implemented to excite guided mode resonance under normal incident light. This leaky mode resonance could be coupled and localized into a thin intrinsic Ge layer with optical stack layers. The nanodisks have a 260 nm height and a 240 nm radius, and they are periodically arranged in the x and y directions, with a period of 720 nm in both directions. Compared to the conventional one dielectric layer, the optical stack layers provide more flexibility in controlling the leaking mode coupling and enable the designer to better confine the light in a thinner Ge waveguide layer and achieve high speed and high efficiency for the proposed device. It is worth mentioning that using Ge as the active layer for transporting the photogenerated carriers will increase the response speed and enhance the −3 dB bandwidths of the device. The sequence layers of our proposed structure can be summarized as SiO_2 substrate, Si layer, Ge thin film, SiO_2 layer, Si_3N_4 layer, Si nanodisks, and Air. The light is incident on the Si nanodisks from above. The Si nanodisks couple the light into the guided mode of the waveguide. The guided mode then propagates through the waveguide and is eventually emitted from the other end of the waveguide. The SiO_2 layer between the Ge and Si_3N_4 layers helps to prevent the light from leaking out of the waveguide. The SiO_2 substrate and the air above also help to prevent the light from leaking out of the waveguide. The proposed structure aims to efficiently guide light by trapping it within the waveguide and minimizing leakage.

The Si nanodisks are used to couple the light into the guided mode of the waveguide because it has a higher refractive index than the surrounding layers. The SiO_2 layer between the Ge and Si_3N_4 layers is used to confine the light in the waveguide because it has a lower refractive index than the surrounding layers. The SiO_2 substrate and the air above are used to prevent the light from leaking out of the waveguide because they have a lower refractive index than the surrounding layers. The specific thickness of each layer in our proposed structure will depend on the desired wavelength of the light and the desired properties of the waveguide.

The thin germanium layer in the proposed structure faces several factors that could lead to higher light absorption: the way light interacts within the layers, the increased interaction time due to confinement, and the influence of the surrounding materials on the electric field. In addition to these phenomena, the specific thickness of the Ge layer can also play a role in enhancing absorption. The optimal thickness for absorption will depend on the wavelength of the incident light and the refractive indices of the surrounding layers. By carefully designing the structure of our proposed device, we can optimize the absorption of light in the thin Ge layer. This could lead to the development of new devices with applications in solar energy, sensing, and communications. The field enhancement in the SiO_2 layer of our proposed structure is primarily attributed to its strategic placement within the multilayer design. Being located at the antinode of the guided mode, where the electric field is strongest, and benefiting from its lower refractive index compared to adjacent layers, the SiO_2 layer facilitates the constructive interference of multiple reflections within the structure. This results in resonance conditions that lead to an enhancement of the electric field within the SiO_2 layer. Additionally, the relatively thin SiO_2 layer further concentrates the field, contributing to the observed enhancement. In summary, the electric field enhancement in the SiO_2 layer is a result of the intricate interplay between interference effects, layer positioning, and the unique properties of the multilayer structure. These two phenomena can overlap due to shared interference principles and layer parameters. Consequently, the SiO_2 layer benefits from the combined effects of both resonances, resulting in the observed field enhancement. This dual-resonance behavior allows for fine-tuning and optimizing the structure's performance for various applications.

Authorized licensed use limited to: Huazhong University of Science and Technology. Downloaded on December 06,2025 at 16:15:11 UTC from IEEE Xplore. Restrictions apply.

B. Simulation

Numerical methods are utilized to investigate the electrical and optical properties of the device as presented in references [28], [29], [30]. In this study, a 3-D finite element method (FEM) is employed to solve Poisson's and drift-diffusion equations using a Newton solver. This approach allows for self-consistent simulation of charge transport and electrical response in the PIN photodetector design. The mesh size is set to a minimum of 10 nm and a maximum of 1 μm with a maximum iteration of 40 for convergence control. To enhance the accuracy of the simulation, the maximum step size in the Germanium layer is set to 9 nm. The 2-D FEM is used to study the temporal behavioral and frequency response of the device. The 3-D finite-difference time-domain (FDTD) method with a periodic boundary condition is used to simulate light propagation in the multilayer structure and study the optical characteristics of the designed photodetector. The time-varying Maxwell's equations are solved using the 3-D-FDTD method, and the frequency analysis is obtained through the Fast Fourier Transform of the FDTD results. The unit cell dimensions are $y = 1440$ nm, $x = 1440$ nm, and $z = 3$ μm, with a mesh size of $\Delta x = \Delta y = 24$ nm and $\Delta z = 26$ nm in the nanodisks, and $\Delta z = 5$ nm in the Germanium layer. Optical and electrical simulations are presented separately in the rest of this paper.

The absorption in the different layer is calculated by

$$P_{\text{abs}}(z) = \frac{1}{2}\omega \text{Im}(\varepsilon)|E(z)|^2 \tag{1}$$

where ω is the angular frequency of the incident light, ε the material permittivity, and $E(z)$ the electric field of exited mode at the different position z. The dark current in a p-i-n photodetector is primarily due to thermal generation of electron-hole pairs in the intrinsic region. A significant simplification can be achieved by modeling the junction as graded, wherein the acceptor and donor concentrations transition smoothly within the depletion region. Under this assumption, the diffusion currents closely resemble those observed in a conventional p-n-junction, albeit with adjusted parameters. The electron (J_n) and hole (J_p) diffusion currents are given by

$$J_n = \frac{q D_{n_{\text{Ge}}} n_{i_{\text{Ge}}}^2}{L_{n_{\text{Ge}}} N_{A_{\text{Ge}}}} \left(e^{\frac{qV}{kT}} - 1\right) \tag{2}$$

$$J_p = \frac{q D_{p_{\text{Si}}} n_{i_{\text{Si}}}^2}{L_{p_{\text{Si}}} N_{D_{\text{Si}}}} \left(e^{\frac{qV}{kT}} - 1\right) \tag{3}$$

where q is the electronic charge, V is the applied bias voltage, k is the Boltzmann's constant, T is the absolute temperature, $D_{n_{\text{Ge}}}$ is Ge's electron diffusion coefficient and $D_{p_{\text{Si}}}$ is Si's hole diffusion coefficient, $n_{i_{\text{Ge}}}$ is the Ge's intrinsic carrier concentration and $n_{i_{\text{Si}}}$ is the Si's intrinsic carrier concentration, $L_{n_{\text{Ge}}}$ is the Ge's electron diffusion lengths and $L_{p_{\text{Si}}}$ is the Si's hole diffusion lengths, and $N_{A_{\text{Ge}}}$ is concentrations of acceptor atoms added to Ge and $N_{D_{\text{Si}}}$ is concentrations of donor atoms added to Si. The total dark current ($J = J_n + J_p$) becomes

$$J = q \cdot \left(\frac{D_{n_{\text{Ge}}} n_{i_{\text{Ge}}}^2}{L_{n_{\text{Ge}}} N_{A_{\text{Ge}}}} + \frac{D_{p_{\text{Si}}} n_{i_{\text{Si}}}^2}{L_{p_{\text{Si}}} N_{D_{\text{Si}}}}\right)\left(e^{\frac{qV}{kT}} - 1\right). \tag{4}$$

TABLE I
TYPICAL PARAMETER VALUES FOR A p-i-n PHOTODIODE AT ROOM TEMPERATURE

Parameter (Symbol)	Si	Ge	Units
Electrons Diffusion Coefficient (D_n)	39	101	cm^2/S
Hole Diffusion Coefficient (D_p)	12	49	cm^2/S
Intrinsic carrier concentration (n_i)	1.05×10^{10}	1.7×10^{13}	cm^{-3}
Electrons Diffusion Length (L_n)	6.245	10.05	μm
Holes Diffusion Length (L_p)	3.464	7	μm

Although this equation offers a concise analytical representation of dark current in a p-i-n heterojunction, a more accurate depiction requires incorporating the influence of bandgap discontinuity, doping profiles, and interface states. This can be achieved by multiplying the general equation by a function (f) that quantifies these effects

$$J_d = J \cdot f\left(\Delta E_g, \text{ doping profiles, interface states}\right) \tag{5}$$

where f is a function that accounts for the effects of bandgap discontinuity, doping profiles, and interface states. Under illumination, the photocurrent generated is given by

$$J_{\text{ph}} = q \cdot \eta \cdot P_{\text{opt}} \cdot \frac{\lambda}{hc} \tag{6}$$

where P_{opt} is the incident light power, η is the quantum efficiency, λ is the wavelength of the incident light, h is Planck's constant, and c is the speed of light. On the other hand, the photocurrent can be calculated by

$$J_{\text{ph}} = q \cdot \eta \cdot G_{\text{opt}} \tag{7}$$

where G_{opt} the generation rate of electron-hole pairs that can be considered equal to the optical power absorbed by the intrinsic Ge layer calculated from (1). Equations (6) and (7) were used to determine the device photocurrent and quantum efficiency. Table I presents the typical value of the parameters used in the simulation.

III. RESULTS AND DISCUSSIONS

In this section, the optical and electrical behavior of the designed device are studied and presented. Our proposed structure comprises the periodic Si nanodisks on optical stacks, a thin Ge layer sandwiched between Si and optical stack layers and the whole SiO_2 substrate. The high refractive Si nanodisks are arranged in the same period in the x and y directions, which can support guided modes under normal incident light. In guided-mode resonance (GMR), the electromagnetic field of the guided mode can leak into underlying dielectric layers and couple light to the thin Ge waveguide layer by optical stacks layer, which leads to enhance electrical field in the Ge layer. The optical stack layers consist of Si_3N_4 and SiO_2 layers, which, compared to conventional one dielectric layer, provides more flexibility in the control and manipulation of the leaking mode coupling and makes the designer able to better confinement of the light in thinner Ge waveguide layer to achieve high speed and high efficiency for the proposed device. The propagation of the light in the multilayer structure is simulated by the 3-D FDTD method with periodic boundary conditions. Calculated absorption spectra of the thin Ge layer

Authorized licensed use limited to: Huazhong University of Science and Technology. Downloaded on December 06,2025 at 16:15:11 UTC from IEEE Xplore. Restrictions apply.

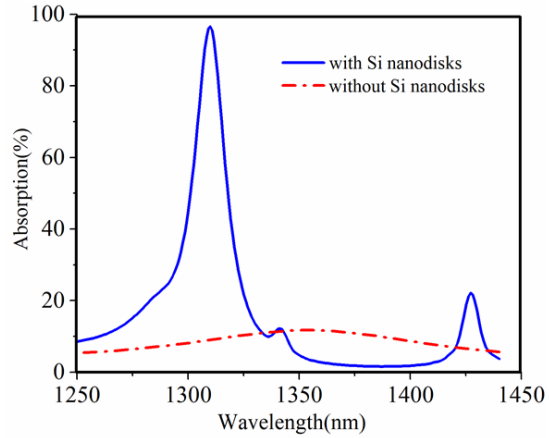

Fig. 2. Calculated absorption spectra of the proposed design with and without Si nanodisks arrays.

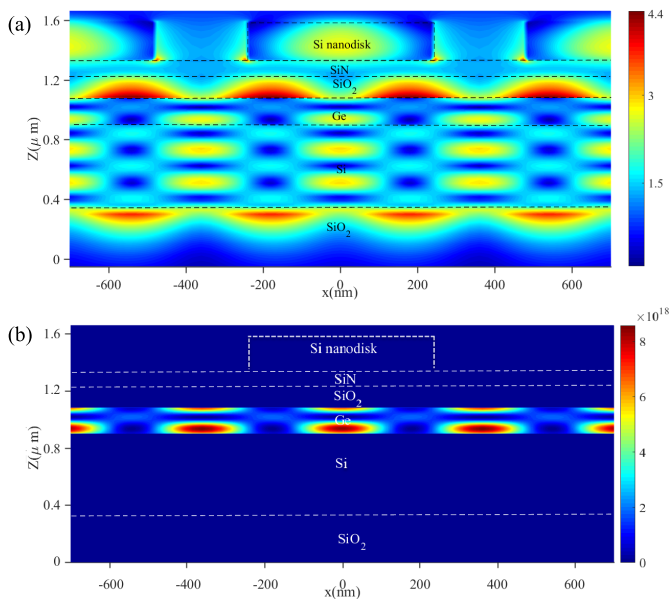

Fig. 3. Detailed optical response of the detector. (a) Profile of the electrical field inside the device in the resonance wavelengths is depicted in Fig. 2. (b) Absorption of incident light in the different layers of the device.

of the proposed structure with and without Si nanodisks array is plotted in Fig. 2. As can be seen, the main absorption peak appeared at a wavelength of 1310 nm in the structure of the Si nanodisks array. The maximum absorption is near 97% of incident light, which is about ten times greater compared to the simple Ge slab without Si nanodisks. The period of the Si nanodisk array and the thickness of optical layers determined the wavelength of the guided mode, which caused the maximum absorption at the wavelength of 1310 nm. The absorption peak in the spectra and its intensity can be manipulated by nanodisk dimensions and geometry.

To further investigate the optical response of the proposed structure, we calculated the detailed electric field distribution and optical absorption inside the structure depicted in Fig. 3(a) and (b), respectively. The electric field profile inside the structure in the x-z plane is plotted in the maximum absorption peak of the resonance wavelength denoted in

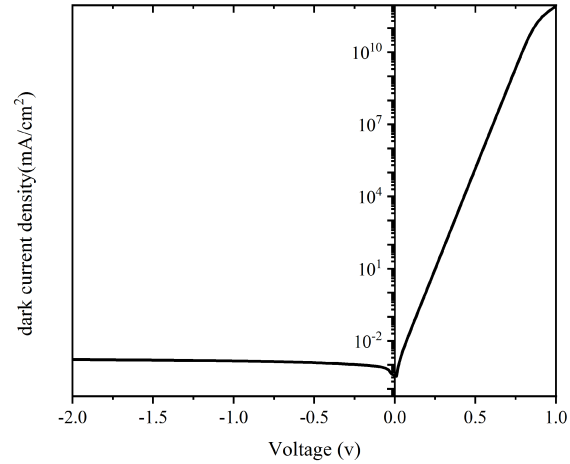

Fig. 4. *I–V* characteristic of the designed device in the dark condition (semi-log scale) for both reverse and forward bias voltages.

Fig. 2. In the resonance wavelength, Si nanodisks have exited the guided mode, and its leaky field has coupled to the Ge slab layer, which has caused the electrical field to increase in the high refractive index Ge slab layer. The field enhancement in the thin absorber Ge layer is the cause of the maximum absorption at the wavelength of 1310 nm. In this layer, as illustrated in Fig. 3(a), more than half of the incident light is concentrated and absorbed in the bottom half of the active Ge layer. This is due to the field enhancement effect caused by the Si nanodisks. The thickness of this region is about 90 nm of the entire Ge layer (180 nm) and matched with the i–Ge region where photo carriers are generated and extracted as electrical current. One advantage of the proposed design is the localization of the incident light in this very thin i-Ge region which can lead to highly sensitive and fast electrical response of the device. The observed field enhancement in the silicon oxide (SiO_2) layers can be related to different reasons. The electric field enhancement in the thin SiO_2 layer above the Si and Ge layers is stronger than the electric field enhancement in the SiO_2 substrate layer. This is because the thin SiO_2 layer is located within the optical stack, where the guided mode and resonance effects are more pronounced. The thin SiO_2 layer is also closer to the Si and Ge layers, which allows for stronger interactions between the incident light, the guided modes, and the SiO_2 layer. As a result, the electric field enhancement in the thin SiO_2 layer is likely influenced by guided-mode resonance and interference effects within the multilayer structure.

The electric field enhancement in the SiO_2 substrate layer is primarily due to interactions with residual fields or evanescent waves that extend beyond the immediate structure. However, these effects are typically weaker than those occurring within the multilayer stack. In summary, the electric field enhancement in the thin SiO_2 layer is stronger than the electric field enhancement in the SiO_2 substrate layer because of its position within the optical stack and its proximity to the Si and Ge layers. Fig. 4 shows a semi-log scale J-V characteristic of the designed PIN Ge-on-Si photodiode. This Figure proves the rectification nature of the device. The passing current through the device grows exponentially in forward bias voltages and

Authorized licensed use limited to: Huazhong University of Science and Technology. Downloaded on December 06,2025 at 16:15:11 UTC from IEEE Xplore. Restrictions apply.

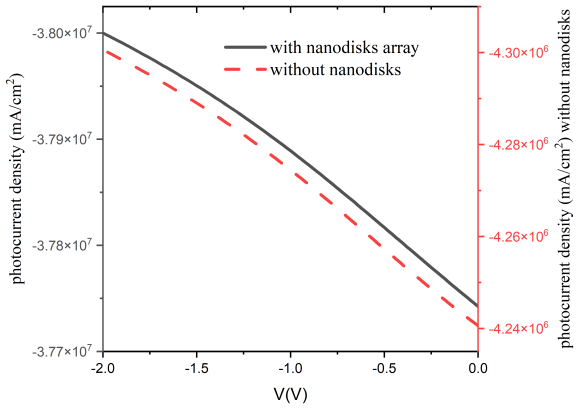

Fig. 5. J–V characteristics of the designed device for both structures, with nanodisks array (left axis) and without nanodisks (right axis) under reverse bias voltages for 1 mW optical power.

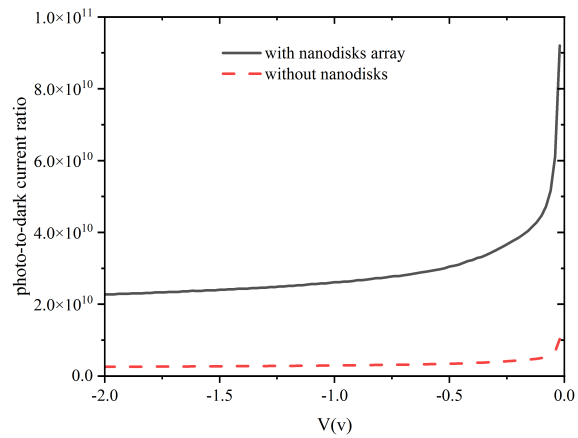

Fig. 6. Photo-to-dark current characteristic of the designed device in the reverse bias voltages for a device with nanodisks array (solid line) and without nanodisks (dashed line) and 1 mW optical power.

gets saturated for the reverse bias voltages. The designed PIN device is biased in the reverse bias for detecting the incident photons. The passing current through the device in the absence of incident light is considered a dark current and plays a noise role in the analysis of device performance. Fig. 4 shows that the device has a dark current density in the order of 10^{-3} mA/cm^2 in the reverse bias. Moreover, the passing current through the device in the presence of incident light is called photocurrent. In Fig. 5, the photocurrent density of the designed Ge-on-Si PIN photodiode is presented versus biasing voltage and compared with the photocurrent density of the traditional design without a silicon nanodisk array. This Figure shows that the designed optical structure increases the photocurrent of the device ∼nine folds. It is worth mentioning that the photo response of the device is calculated for 1 mW optical power, and the temporal behavior and frequency response are studied for 0.5 mW optical power. The photo-to-dark current ratio is an important parameter in the design of photodetectors' readout circuits. This ratio reflects the sensitivity of the photodetector in low-level light conditions. It is defined as the ratio of the photocurrent generated by the photodetector, when exposed to light, to the dark current that flows through the device even in complete darkness. The higher the ratio, the better the photodetector's ability to detect low light levels. Readout circuits are designed to amplify the small electrical signals generated by the photodetector and convert them into electrical data. To achieve high-quality and reliable data, it is important to minimize the noise in the readout circuit. The noise in the circuit is a combination of the noise generated by the photodetector and the noise generated by the readout circuit. By optimizing the photo-to-dark current ratio, it is possible to reduce the noise generated by the photodetector and, therefore, improve the overall performance of the readout circuit. Therefore, the photo-to-dark current ratio is an important parameter that is taken into consideration when designing readout circuits. The photo-to-dark current ratio is an important parameter that identifies the ability of a photodiode to separate an output electrical signal (photocurrent) from a noise signal (dark current). Fig. 6 presents the photo-to-dark current ratio of the designed device with optical structure compared with a structure without silicon nanodisks array. From this Figure, the device has a photo-to-dark current ratio of 3×10^{10} in -0.5 volt biasing voltage, which is larger than the best report in the literature (Table I). Moreover, this Figure shows that the designed optical structure and silicon nanodisk resulted in a ninefold improvement in the photo-to-dark current ratio of the device. The photo-to-dark current ratio of the device is usually a voltage-dependent parameter because of dark current variation with biasing voltage. Therefore, it is necessary to know the nature of the photo-to-dark current ratio with biasing voltage. Fig. 6 provides the photo-to-dark current ratio of the device versus reverse bias voltage. From the data provided in this Figure, the photo-to-dark current ratio of about 10^{11} values can also be achieved by this device for very small bias voltages, but the parameter is sensitive to the biasing voltage. On the other hand, for a little more biasing voltage, the photo-to-dark current ratio reduces from its initial value but gets saturated with damped sensitivity to the biasing voltage.

Self-powered photodetectors represent a critical advancement in the field, eliminating the need for an external power source. This unique characteristic makes them ideal for applications where traditional power supplies are limited or entirely absent. Notably, one of the key strengths of this design is its inherent self-driven operation. Fig. 7 shows the photocurrent of the designed Ge-on-Si PIN photodiode in the self-driven mode for both structures, with silicon nanodisk arrays and without nanodisks. This Figure illustrates that the photodiode with silicon nanodisk arrays provides an open-circuit voltage of 0.65 V ($V_{oc} = 0.65$ V), and a short-circuit photocurrent density of 3.77×10^7 mA/cm^2 ($J_{sc} = 3.77 \times 10^7$ mA/cm^2) when exposing to the photon at wavelength of 1310 nm with 1 mW optical power, while the device without nanodisks array has $V_{oc} = 0.58$ V and $J_{sc} = -4.24 \times 10^6$ mA/cm^2. This Figure clearly proves the ability of the designed device for light conversion to detectable electrical signal without any external bias and the advantage of silicon nanodisk arrays in enhancing the short-circuit photocurrent.

As mentioned before, the main aim of this research is to design a high-performance photodiode for working in

Authorized licensed use limited to: Huazhong University of Science and Technology. Downloaded on December 06,2025 at 16:15:11 UTC from IEEE Xplore. Restrictions apply.

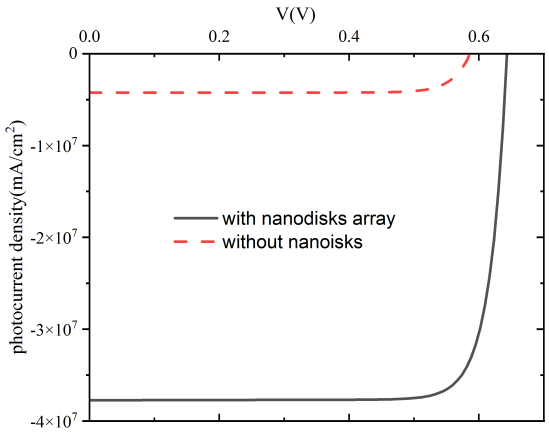

Fig. 7. Photocurrent characteristic of the designed device under forward bias voltages for the device with optical structure and without silicon nanodisks array at $\lambda = 1310$ nm and 1 mW optical power.

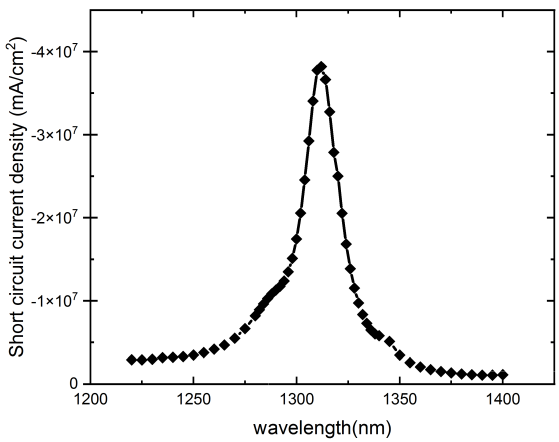

Fig. 8. Short-circuit photocurrent density of the device for different wavelengths at 1 mW optical power.

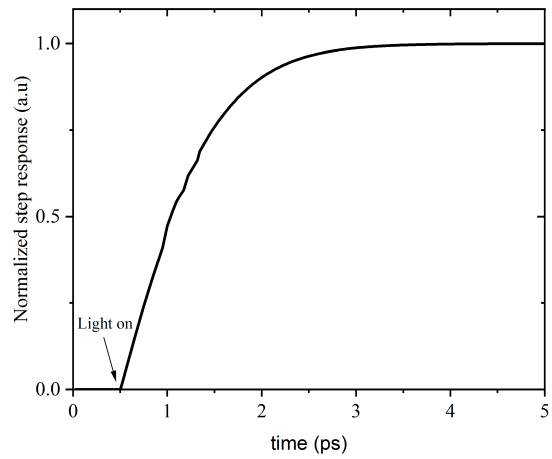

Fig. 9. Temporal response of the designed device (with the surface area of $10 \times 10\ \mu m^2$) to an optical step pulse with 0.5 mW optical power at 1310 nm wavelength.

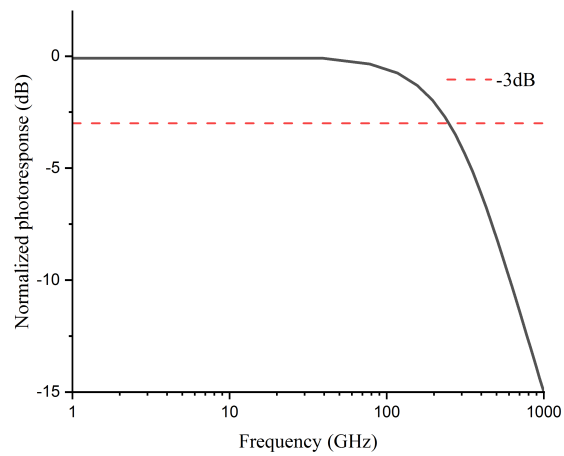

Fig. 10. Frequency response of the designed device (with the surface area of $10 \times 10\ \mu m^2$) for 0.5 mW optical power at 1310 nm wavelength.

the o-band, especially in $\lambda = 1310$ nm. The carefully designed optical structure serves a dual purpose: trapping the desired light within the photodiode's light-absorbing region and filtering out unwanted wavelengths. This maximizes light absorption for the target signal. The optical characteristics of the device presented in Figs. 2 and 3 prove the achievement of these two goals. The designed device's performance is evaluated by calculating its photocurrent response across various wavelengths. This data is then plotted in Fig. 8 to see if it meets the research objectives. This Figure proves the agreement between electrical and optical characteristics of the device.

The temporal response of a photodetector refers to its ability to respond to changes in incident light over time. This includes both the speed at which the detector responds to changes in light intensity and the duration of the response. The temporal response of a photodetector is typically characterized by its rise time, fall time, and bandwidth. The rise time is the time it takes for the detector to go from 10% to 90% of its final output in response to a step change in incident light. The fall time is the time it takes for the detector to return to 10% of its final output in response to a step change in incident light. The bandwidth is the range of frequencies over which the detector can respond to changes in incident light. Several approaches are used to design a PIN photodetector with a faster response time. This can be achieved by reducing the travel distance for generated charges, optimizing material properties (modifying the doping concentration of the semiconductor material and enhancing the drift velocity of the photocarriers), improving internal electric fields, minimizing internal delays (reducing the parasitic capacitance), and optimizing light reception (improving the optical coupling).

Here, we used Ge as an active material for light absorption because of its better carriers' mobility and higher optical absorption (in O-band) over Si, which improved the temporal response of the designed device. Moreover, the carriers' transit time is reduced by decreasing the thickness of the i-region while keeping the optical characteristic with the aid of a silicon nanodisk array and optical structure, and the doping concentration is tried to be optimized to achieve the goal. Fig. 9 presents the response time of the designed photodiode at 0 V (self-powered). The response time of this photodiode was found to be 1.4 ps, which is an excellent candidate for ultrahigh-speed optical communication in O-band. It is worth noting that the

Authorized licensed use limited to: Huazhong University of Science and Technology. Downloaded on December 06,2025 at 16:15:11 UTC from IEEE Xplore. Restrictions apply.

temporal characteristic of a photodiode directly depends on the area of the device. In this study, a 10×10 μm^2 device was illuminated by a 0.5 mW light source at the wavelength of 1310 nm. The key takeaway is that the frequency response of a photodetector describes how well it picks up on changes in light intensity at frequencies. This response is characterized by two things: bandwidth and rise/fall times. Bandwidth tells the spread of speeds the detector can handle, and rise/fall times tell you how quickly it reacts to a sudden change in light intensity.

In PIN photodetectors, a critical design consideration is the interplay between active area and -3 dB bandwidth. While enlarging the active area initially improves performance, this benefit reaches a saturation point. Increased area facilitates greater photon capture, enhancing the signal-to-noise ratio and overall sensitivity. However, this advantage diminishes beyond a certain size due to a concomitant rise in junction capacitance. This capacitance impedes response time, ultimately limiting the maximum operational frequency, or bandwidth, of the photodetector. In this research, the device is proposed to have 10×10 μm area. Fig. 10 provides the frequency response of the designed Ge-on-Si photodetector. The designed device has a -3 dB cutoff frequency of 250 GHz. This cutoff frequency is much greater than the reported Ge-based photodetectors, which can revolutionize the optical communication in O-band. Mobility saturation can significantly impact the performance of a PIN photodiode, particularly in applications where high speed and linearity are critical. When mobility saturation occurs, the response of the photodiode becomes nonlinear, which can lead to distortion in the output signal. In terms of frequency response, mobility saturation can limit the bandwidth of the photodiode. In this study, the carriers' mobility saturation model is considered for better evaluation of response time and frequency response. Table II provides a detailed comparison between the important parameters of the design Ge-on-Si PIN photodetector with the reported Ge-based photodetector in literature. Our device achieves an EQE of 74% and responsivity of 0.78 A/W at 1310 nm, which compares favorably to other Ge-on-Si photodetectors. For example, Lin et al. [24] reported a vertical Ge-on-SiO_2 PIN photodetector with a responsivity of 0.39 A/W at 1550 nm. Our design's higher responsivity can be attributed to the efficient light coupling provided by the silicon nanodisk array. In terms of speed, our device exhibits an exceptional response time of 1.4 ps and a -3 dB bandwidth of 250 GHz. This surpasses the performance of many existing designs, such as the Ge-on-Si photodetector by Xiao Hu et al. [26] which achieved a -3 dB bandwidth of 60 GHz The ultra-thin Ge layer in our design contributes significantly to this high-speed performance. Our device's high photo-to-dark current ratio of 3×10^{10} is particularly noteworthy. This significantly outperforms many conventional photodetectors and is crucial for low-noise operation. The device has a very fast response speed compared to all the reported devices. The best-reported response time is in the order of several nanoseconds [31], but the design device's response time is in the order of Pico seconds. The device has an EQE of 74% while the best reported EQE is 51.5% [25]. The device has a -3 dB bandwidth of 250 GHz while the best reported -3 dB bandwidth is 48 GHz [14]. While our work focuses on guided-mode resonance, it is worth noting that other approaches, such as plasmonic enhancement, quantum structure infrared photodetectors, and novel materials for IR detection have also been explored to improve photodetector performance [36], [37], [38]. In developing a Guided-Mode Resonance Enhanced Ge-on-Si Photodetector, addressing elaboration costs is crucial for practical viability. Our design uses abundant materials, integrates with CMOS technology, and operates self-driven, minimizing costs. While validation requires resources, the combination of low material costs, reduced operational expenses, and compatibility with established fabrication techniques positions our photodetector as a cost-effective solution for high-speed optical communication systems. By carefully considering these factors, we aim to ensure that our technology is not only innovative but also practical and competitive in the rapidly evolving field of optical communications.

TABLE II
COMPARISON BETWEEN THE PERFORMANCE OF DIFFERENT STRUCTURES OF PIN Ge-ON-Si PHOTODETECTORS OPERATING AT 1310 nm

Scheme	I_{ph}/I_d	R (A/W)	EQE (%)	BW (GHz)	Ref
Ge-on-Si	4.33×10^4	0.54	51.5		[25]
Ge-on-SOI	1.13×10^5	0.59	-	48	[32]
Ge-on-Si	10^5	0.275	26	-	[33]
Ge-on-Si	4.04×10^2	0.52	-	4.14	[34]
Ge-on-Si	2×10^3	0.22	-	-	[35]
Ge-on-Si	3×10^{10}	0.78	74	250	This work

IV. CONCLUSION

We have demonstrated a high-performance self-powered photovoltaic Ge-on-Si PIN photodiode for operation in the O-band (1310 nm) of the optical communication spectrum. This design addresses the challenge of low light absorption in Ge by incorporating a periodic array of silicon nanodisks. These nanodisks effectively localize incident light within a very thin (100 nm) Ge absorption layer, achieving high light–matter interaction through guided-mode resonance. This approach not only significantly enhances the EQE to 74% and responsivity to 0.78 A/W but also enables a remarkable response time of 1.4 ps. Furthermore, the confinement of light and the thin absorption layer contributes to a high photo-to-dark current ratio (3×10^{10}) and a broad -3 dB bandwidth of 250 GHz, exceeding previously reported values for Ge photodetectors in this wavelength range. This combination of high efficiency, ultrafast response, and miniaturized design paves the way for next-generation high-speed near-infrared photodetectors.

REFERENCES

[1] Z. Li, T. Yan, and X. Fang, "Low-dimensional wide-bandgap semiconductors for UV photodetectors," *Nature Rev. Mater.*, vol. 8, no. 9, pp. 587–603, 2023.

[2] T. Yan, W. Yang, L. Wu, and X. Fang, "High-work-function transparent electrode with an enhanced air-stable conductivity based on AgNiCu core-shell nanowires for Schottky photodiode," *J. Mater. Sci. Technol.*, vol. 209, pp. 95–102, Feb. 2025.

Authorized licensed use limited to: Huazhong University of Science and Technology. Downloaded on December 06,2025 at 16:15:11 UTC from IEEE Xplore. Restrictions apply.

[3] Y. Chen, L. Su, M. Jiang, and X. Fang, "Switch type PANI/ZnO core-shell microwire heterojunction for UV photodetection," *J. Mater. Sci. Technol.*, vol. 105, pp. 259–265, Apr. 2022.

[4] H. D. Jahromi and A. Zarifkar, "A physical model for quantum wire infrared photodetectors under illumination condition," *Opt. Commun.*, vol. 493, Aug. 2021, Art. no. 127043.

[5] J. Huang et al., "Midwave infrared quantum dot quantum cascade photodetector monolithically grown on silicon substrate," *J. Lightw. Technol.*, vol. 36, no. 18, pp. 4033–4038, Sep. 15, 2018.

[6] H. D. Jahromi, A. Binaie, M. H. Sheikhi, A. Zarifkar, and H. Nadgaran, "Response of colloidal quantum dot infrared photodetectors to modulated optical signals," *IEEE Sensors J.*, vol. 15, no. 6, pp. 3274–3280, Jun. 2015.

[7] P. Xiao et al., "Solution-processed 3D RGO–MoS_2/pyramid Si heterojunction for ultrahigh detectivity and ultra-broadband photodetection," *Adv. Mater.*, vol. 30, no. 31, Aug. 2018, Art. no. 1801729.

[8] S. Li et al., "The O-band 20-channel 800 GHz arrayed waveguide grating based on silica platform for 1 Tb/s or higher-speed communication system," *Opt. Laser Technol.*, vol. 156, Dec. 2022, Art. no. 108475.

[9] J. Zhang, X. Gong, H. Zhang, and Y. Yang, "Design and analysis of p-i-n-type MoS_2/Ge heterojunction photodetector," *IEEE Trans. Electron Devices*, vol. 69, no. 12, pp. 6865–6870, Dec. 2022.

[10] H. D. Jahromi, A. Mahmoodi, M. H. Sheikhi, and A. Zarifkar, "Spectral response, dark current, and noise analyses in resonant tunneling quantum dot infrared photodetectors," *Appl. Opt.*, vol. 55, no. 30, p. 8494, 2016.

[11] X. Li et al., "Comparative study on dark current mechanisms of n-on-p and p-on-n long-wavelength HgCdTe infrared detectors," *Infr. Phys. Technol.*, vol. 123, Jun. 2022, Art. no. 104166.

[12] P. Bai et al., "Broadband and photovoltaic THz/IR response in the GaAs-based ratchet photodetector," *Sci. Adv.*, vol. 8, no. 21, May 2022, Art. no. eabn2031.

[13] F. Yang et al., "Ultrathin broadband germanium–graphene hybrid photodetector with high performance," *ACS Appl. Mater. Interface*, vol. 9, no. 15, pp. 13422–13429, 2017.

[14] C. Li, B. Li, S. Qin, J. Su, X. He, and X. Guo, "Effects of interface states on Ge-On-SOI photodiodes," *IEEE J. Electron Devices Soc.*, vol. 7, pp. 7–12, 2019.

[15] S. Mauthe et al., "High-speed III–V nanowire photodetector monolithically integrated on Si," *Nature Commun.*, vol. 11, no. 1, p. 4565, Sep. 2020.

[16] E. M. T. Fadaly et al., "Direct-bandgap emission from hexagonal Ge and SiGe alloys," *Nature*, vol. 580, no. 7802, pp. 205–209, Apr. 2020.

[17] S. A. Srinivasan et al., "56 Gb/s NRZ O-band hybrid BiCMOS-silicon photonics receiver using Ge/Si avalanche photodiode," *J. Lightw. Technol.*, vol. 39, no. 5, pp. 1409–1415, Mar. 15, 2021.

[18] Y. Yuan et al., "64 gbps PAM4 Si-Ge waveguide avalanche photodiodes with excellent temperature stability," *J. Lightw. Technol.*, vol. 38, no. 17, pp. 4857–4866, Sep. 15, 2020.

[19] R. M. Saadabad, L. Huang, and A. E. Miroshnichenko, "Polarization-independent perfect absorber enabled by quasibound states in the continuum," *Phys. Rev. B, Condens. Matter*, vol. 104, no. 23, Dec. 2021, Art. no. 235405.

[20] Z. Liu et al., "Enhanced light trapping in Ge-on-Si-on-insulator photodetector by guided mode resonance effect," *J. Appl. Phys.*, vol. 124, no. 5, Aug. 2018, Art. no. 053101.

[21] A. Dorodnyy et al., "Plasmonic photodetectors," *IEEE J. Sel. Topics Quantum Electron.*, vol. 24, no. 6, pp. 1–13, Nov. 2018.

[22] A. I. Yakimov, V. V. Kirienko, A. A. Bloshkin, A. V. Dvurechenskii, and D. E. Utkin, "Mid-infrared optical resonances in quantum dot photodetectors coupled with metallic gratings with different aperture diameters," *Current Appl. Phys.*, vol. 20, no. 7, pp. 877–882, Jul. 2020.

[23] L.-Q. Chen et al., "High-performance ge p-i-n photodetector on Si substrate," *Optoelectronics Lett.*, vol. 11, no. 3, pp. 195–198, May 2015.

[24] Y. Lin et al., "High-efficiency normal-incidence vertical p-i-n photodetectors on a germanium-on-insulator platform," *Photon. Res.*, vol. 5, no. 6, p. 702, 2017.

[25] X. Zhao et al., "High performance p-i-n photodetectors on Ge-on-Insulator platform," *Nanomaterials*, vol. 11, no. 5, p. 1125, Apr. 2021.

[26] X. Hu et al., "High-speed and high-power germanium photodetector with a lateral silicon nitride waveguide," *Photon. Res.*, vol. 9, no. 5, p. 749, 2021.

[27] H. Zhou et al., "Grating and hole-array enhanced germanium lateral p-i-n photodetectors on an insulator platform," *Opt. Exp.*, vol. 30, no. 4, p. 4706, 2022.

[28] H. D. Jahromi and A. Lotfiani, "A fast and sensitive Schottky photodiode with surface plasmon enhanced photocurrent and extremely low dark current for high-frequency applications in near-infrared," *IEEE Sensors J.*, vol. 22, no. 21, pp. 20430–20437, Nov. 2022.

[29] A. Lotfiani, H. D. Jahromi, and S. Hamedi, "Monolithic silicon-based photovoltaic-nanoplasmonic biosensor with enhanced limit of detection and minimum detectable power," *J. Lightw. Technol.*, vol. 40, no. 4, pp. 1231–1237, Feb. 15, 2022.

[30] M. Doriani, H. D. Jahromi, and M. H. Sheikhi, "A highly efficient thin film $CuInGaSe_2$ solar cell," *J. Sol. Energy Eng.*, vol. 137, no. 6, Dec. 2015, Art. no. 064501.

[31] Q. Y. Zeng et al., "Photovoltaic field effect transistor (PVFET)-based Ge/Si photodetector for low-power silicon photonics," *AIP Adv.*, vol. 9, no. 8, Aug. 2019, Art. no. 085226.

[32] Z. Liu et al., "48 GHz high-performance Ge-on-SOI photodetector with zero-bias 40 gbps grown by selective epitaxial growth," *J. Lightw. Technol.*, vol. 35, no. 24, pp. 5306–5310, Dec. 15, 2017.

[33] A. Aliane et al., "Fabrication and characterization of sensitive vertical P-i-N germanium photodiodes as infrared detectors," *Semiconductor Sci. Technol.*, vol. 35, no. 3, Mar. 2020, Art. no. 035013.

[34] X. Li et al., "High-power back-to-back dual-absorption germanium photodetector," *Opt. Lett.*, vol. 45, no. 6, p. 1358, 2020.

[35] P.-H. Huang, C.-H. Chou, and C.-L. Hsin, "Ge photodetector monolithically integrated on Si by rapid-melting-growth technique," *IEEE Photon. Technol. Lett.*, vol. 27, no. 12, pp. 1254–1256, Jun. 1, 2015.

[36] N. Zeiri, S. Abdi-Ben Nasrallah, N. Sfina, and M. Said, "Modeling of electrical and optical characteristics of near room-temperature CdS/ZnSe based NIR photodetectors," *Infr. Phys. Technol.*, vol. 64, pp. 33–39, May 2014.

[37] A. R. Izadpour, H. D. Jahromi, and M. H. Sheikhi, "Plasmonic enhancement of colloidal quantum dot infrared photodetector photosensitivity," *IEEE J. Quantum Electron.*, vol. 54, no. 3, pp. 1–7, Jun. 2018.

[38] S. Ghosh, B. Mukhopadhyay, G. Sen, and P. K. Basu, "Performance analysis of GeSn/SiGeSn quantum well infrared photodetector in terahertz wavelength region," *Phys. E, Low-Dimensional Syst. Nanostruct.*, vol. 115, Jan. 2020, Art. no. 113692.

Ahmad Lotfiani received the Ph.D. degree in photonics from Shahid Beheshti University, Tajrish, Iran, in 2020.

Currently, he serves as an Assistant professor in the Electrical Engineering Department at Jahrom University. His research focuses on developing innovative optoelectronic sensors and exploring the frontiers of quantum photonics.

Hamed Dehdashti Jahromi received the B.Sc. degree from the University of Tabriz, Tabriz, Iran, in 2007, and the M.Sc. and Ph.D. degrees in electronics engineering from Shiraz University, Shiraz, Iran, in 2010 and 2015, respectively.

He was a Research Assistant at the Research Laboratory for Fabrication of Advanced Semiconductor Devices at Shiraz University, from 2014 to 2016. He joined Jahrom University, Jahrom, Iran, in 2016, where he is now an Associate Professor at the Faculty of Engineering. His research interests include photonic devices, nano-optoelectronics, and nanoelectronic devices, especially nanodetectors, such as nanoparticle-based photodetectors, SOAs, optical gates, and nanoscale solar cells.

Authorized licensed use limited to: Huazhong University of Science and Technology. Downloaded on December 06,2025 at 16:15:11 UTC from IEEE Xplore. Restrictions apply.